Solvent Effects on the $O_2(a^1\Delta_g)-O_2(X^3\Sigma_g^-)$ Radiative Transition: Comments Regarding Charge-Transfer Interactions

Tina D. Poulsen and Peter R. Ogilby*

Department of Chemistry, Aarhus University, Langelandsgade 140, 8000 Aarhus, Denmark

Kurt V. Mikkelsen*

Department of Chemistry, H. C. Ørsted Institute, University of Copenhagen, Universitetsparken 5, 2100 Copenhagen, Denmark

Received: June 9, 1998; In Final Form: August 7, 1998

Gas-phase vertical ionization potentials for 27 molecules have been corrected to account for the effects of solvation. Values thus modified do not correlate well with rate constants, k_r^{a-X}, for the solution-phase $O_2(a^1\Delta_g)-O_2(X^3\Sigma_g^-)$ radiative transition. The data are, therefore, not in accord with a proposed model in which charge-transfer interactions are said to be a principal factor in the effect of the solvent on the $O_2(a^1\Delta_g)-O_2(X^3\Sigma_g^-)$ transition probability. The trend in plots of k_r^{a-X} against the ionization potential (IP) is shown, rather, to reflect a transitive effect, deriving from relationships between (1) k_r^{a-X} and the solvent refractive index, n, and (2) n and IP. Using data recorded in 56 solvents, k_r^{a-X}/n^2 is shown to depend linearly on n or functions of n, such as the solvent optical polarizability.

Introduction

The effect of solvent on radiative transitions in molecular oxygen remains a subject of great interest.[1−8] Of special concern is the $O_2(a^1\Delta_g)-O_2(X^3\Sigma_g^-)$ transition, hereafter denoted $a-X$, which is forbidden in the isolated molecule but becomes $\sim 10^4$ times more probable due to solvent perturbations. Solvent-dependent differences in the $a-X$ radiative rate constant, k_r^{a-X}, are likewise pronounced and can exceed a factor of 20.[1−8] To elucidate events that influence k_r^{a-X}, attempts have been made to identify the solvent parameters with which the changes in k_r^{a-X} best correlate.

It is well-documented that in the oxygen−organic molecule (M) photosystem, the $M-O_2$ charge-transfer (CT) state, $M^{+\bullet}O_2^{-\bullet}$, plays an important role.[9−15] There is certainly sufficient evidence to indicate that $O_2(a^1\Delta_g)$ and $O_2(X^3\Sigma_g^-)$ can be indirectly coupled through the CT state.[13,16−18] Although the CT state can be comparatively high in energy, particularly for molecules typically used as solvents, admixture of CT character into the lower-lying valence states $M-O_2(a^1\Delta_g)$ and $M-O_2(X^3\Sigma_g^-)$ could enhance the $a-X$ transition and give rise to solvent-dependent changes in k_r^{a-X}. The extent to which the CT state would perturb the lower energy valence states would depend on the energy of the CT state, among other things. Assuming that the effect of the counterion, $O_2^{-\bullet}$, does not change appreciably from one solvent to the next, it is thus reasonable to examine how experimental k_r^{a-X} data correlate to changes in the ionization potential of M.

Proponents of the CT-coupling postulate claim a linear correlation when functions of k_r^{a-X} are plotted against the gas-phase ionization potential of M.[5,19] Although a general trend can indeed be discerned in such plots, the data are scattered and the claim of a linear correlation is questionable. To more properly test this CT postulate, one should rather consider ionization potentials that reflect the effects of both equilibrium and nonequilibrium solvation. The results of such a study are reported herein.

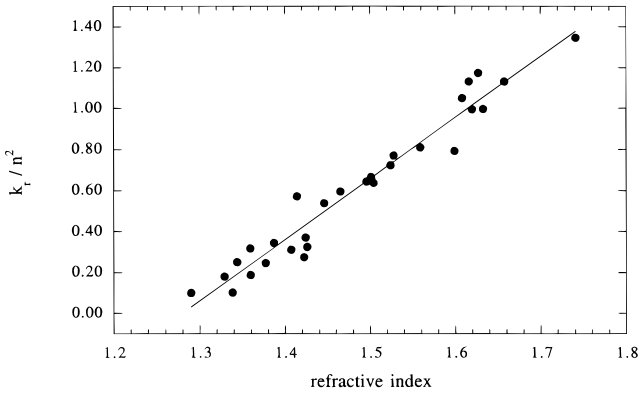

Figure 1. Plot of k_r^{a-X}/n^2 vs the solvent refractive index, n. For this plot, relative k_r^{a-X} values[2] have been normalized to yield $k_r^{a-X} = 1.5$ s^{-1} in benzene[3] (Table 1). The solid line is a linear least-squares fit to the data. An equally good correlation is observed when k_r^{a-X}/n^2 is plotted against functions of n, such as the solvent polarizability $[(n^2 - 1)/(n^2 + 2)]$.

Results and Discussion

For any molecule, the rate constant for a radiative transition will depend intrinsically on the solvent. This dependence is embodied by the appearance of the square of the solvent refractive index, n, in the expression of the Einstein coefficient, A, for spontaneous emission from an upper to lower state (eq 1, where Γ is the integrated absorption coefficient in M^{-1} cm^{-2}, ν the transition frequency in cm^{-1}, and g the degeneracy of the given state).[20]

$$A = k_r = n^2 \frac{8\pi c \ln(10)}{N_A} \frac{g_{lower}}{g_{upper}} \nu^2 \Gamma \qquad (1)$$

* To whom correspondence should be addressed

10.1021/jp982567w CCC: $15.00
Published on Web 10/21/1998

TABLE 1: Nonequilibrium Molecular Ion Solvation Energies (E^{neq}) and Cohesive Energies (U) Used To Correct the Gas-Phase Vertical Ionization Potential, IP^{gas}, for the Effects of Solvation

solvent	n	k_r^{a-X} (s^{-1})	r_c[a] (Å)	E^{neq} (kJ/mol)	U (kJ/mol)	$E^{neq} - U$ (kJ/mol)	IP^{gas} (kJ/mol)	IP^{sol} (kJ/mol)
CF_3CH_2OH	1.2900	0.165	3.05	90.8	*b*		1129	
methanol	1.3290	0.315	2.45	122.9	35.7	87.2	1047	959.8
water-d_2	1.3384	0.180	1.90	161.2	41.3	119.9	1219	1099
acetonitrile	1.3438	0.450	2.84	109.2	31.1	78.1	1177	1099
acetone	1.3590	0.585	3.04	104.9	28.9	76.0	937.9	861.9
ethanol-O_d	1.3595	0.345	3.06	104.3	40.0	64.3	1012	947.7
2-propanol	1.3770	0.465	3.08	106.6	42.8	63.8	976.5	912.7
n-heptane	1.3870	0.660	4.53	73.6	34.1	39.5	957.2	917.7
THF	1.4070	0.615	3.13	109.8	29.5	80.3	907.9	827.6
trifluorotoluene	1.4140	1.14	4.67	74.4	35.2	39.2	934.5	895.3
1,4-dioxane	1.4220	0.555	3.24	108.4	36.1	72.3	886.7	814.4
dichloromethane	1.4241	0.750	2.96	119.2	26.3	92.9	1092	999.1
cyclohexane	1.4260	0.660	3.34	105.6	30.5	75.1	951.4	876.3
chloroform	1.4460	1.13	3.13	115.8	28.8	87.0	1097	1010
fluorobenzene	1.4650	1.28	3.74	99.2	32.4	66.8	887.7	820.9
toluene	1.4960	1.44	3.84	100.1	35.6	64.5	852.0	787.5
benzene	1.5010	1.50	3.28	117.7	31.4	86.3	892.1	805.8
1-iodopropane	1.5040	1.44	4.62	83.8	33.8	50.0	916.6	866.6
chlorobenzene	1.5240	1.68	4.13	95.7	38.8	56.9	874.2	817.3
benzonitrile	1.5280	1.80	4.17	95.3	35.3	60.0	939.8	879.8
bromobenzene	1.5590	1.97	4.75	86.1	43.2	42.9	866.5	823.6
2-ethylnaphthalene	1.5994	2.03	5.56	76.1	60.0[c]	16.1	767.1	751.0
1,3-dibromobenzene	1.6083	2.72	4.32	98.5	59.7[c]	38.8	875.1	836.3
1-methylnaphthalene	1.6160	2.96	4.45	96.4	60.3	36.1	772.9	736.8
iodobenzene	1.6200	2.61	5.16	83.3	59.4	23.9	843.3	819.4
carbon disulfide	1.6270	3.11	3.07	140.7	25.1	115.6	971.6	856.0
diphenyl sulfide	1.6327	2.66	5.46	79.5	*b*		758.4	
1-bromonaphthalene	1.6575	3.11	5.72	77.3	61.2	16.1	779.6	763.5
diiodomethane	1.7411	4.08	3.25	143.1	46.8	96.3	912.8	816.5

[a] 10% smaller than the estimated upper limit for the cavity radius, r_c (see text). [b] Available information was insufficient to provide an accurate estimate. [c] Estimated.

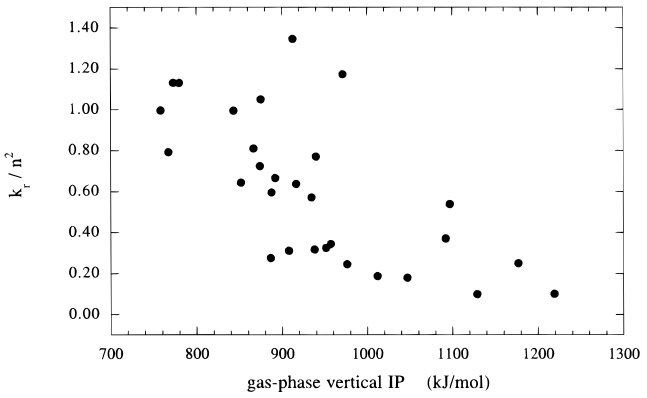

Figure 2. Plot of k_r^{a-X}/n^2 against the gas-phase vertical ionization potential, IP^{gas}, for the respective solvents. Values for k_r^{a-X} and IP^{gas} are listed in Table 1.

The solvent-dependence of k_r^{a-X} actually observed, however, is much larger than that "expected" based only on eq 1. This is illustrated in Figure 1, where values of k_r^{a-X}/n^2 are plotted against n. This comparatively large dependence of k_r^{a-X} on solvent is sufficient to justify models based on a "complex" between oxygen and a solvent molecule, including the CT-based model.

A plot of these k_r^{a-X}/n^2 data against the gas-phase vertical ionization potential, IP^{gas}, of the corresponding solvent molecule is shown in Figure 2.[21] Although a general trend is apparent, the correlation is not particularly good. Clearly, an abscissa that better represents the energy of the $M^{+\bullet}O_2^{-\bullet}$ state in solution is desirable. Unfortunately, it is difficult to obtain experimental ionization potentials for a wide range of solutes M in a solvent of like molecules M.[22] Although oxidation potentials reflect the stability of the ion $M^{+\bullet}$ *in equilibrium* with the solvent, such data could nevertheless potentially be useful in assessing the energy of the $M-O_2$ CT state. Unfortunately, it is likewise difficult to obtain such data for the molecules listed in Table 1. A more tractable approach to this problem is to use computational methods to estimate the effects of solvation on IP^{gas}.[23]

For each molecule M, we obtained the solution-phase complement of IP^{gas} by using (1) the cohesive energy, U, to account for the stabilization of the ground-state neutral M (equilibrium solvation)[24] and (2) nonequilibrium solvation theories to estimate the energy of the $M^{+\bullet}$ Franck−Condon state in a medium composed of M.[25−28] Use of a nonequilibrium solvation model for $M^{+\bullet}$ is also appropriate given that the $M-O_2$ CT state lifetime is short and on the order of the solvent reorganization time.[29−31] The nonequilibrium solvation energy, E^{neq}, for the ion was obtained from the expression

$$E^{neq} = \frac{1}{2\,r_c}\left(1 - \frac{1}{n^2}\right) \qquad (2)$$

where r_c is the radius of a spherical solvent cavity housing M and n is the solvent refractive index.[25] The modified ionization potential, IP^{sol}, was obtained by adding U and subtracting E^{neq} from IP^{gas}.

For each molecule, an upper limit for the cavity radius, r_c^{max}, was obtained in the following manner: (1) An equilibrium nuclear geometry was calculated using the molecular mechanics part of the SPARTAN[32] program package, (2) the molecular center-of-mass was then determined, (3) the distance, d, from the center-of-mass to the most distal nucleus was obtained, and (4) the van der Waals radius of that particular distal nucleus was added to d.

The assumption of a spherical solvent cavity, however, has its limitations. In an attempt to mitigate errors associated with

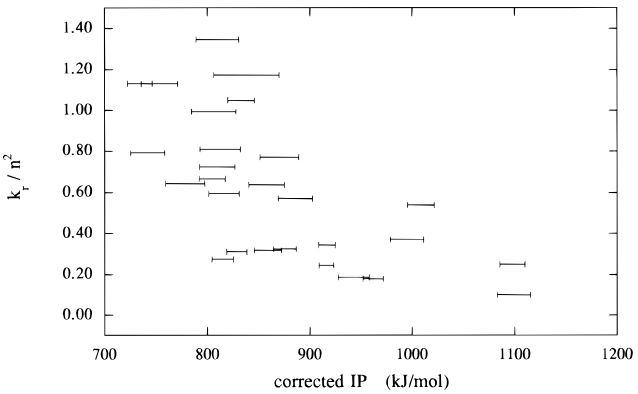

Figure 3. Plot of k_r^{a-X}/n^2 against IP^{sol}, the ionization potential modified for the effects of solvation. For each value of k_r^{a-X}/n^2, a range of IP^{sol} values is designated. The right-side boundary derives from calculations using r_c^{max}, whereas the left-side boundary derives from calculations using r_c^{min}.

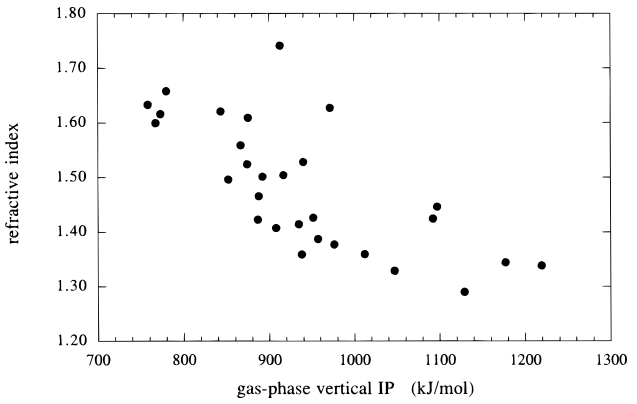

Figure 4. Plot of the refractive index against IP^{gas} for the respective solvents.

this assumption, values of IP^{sol} were calculated for a range of cavity radii. The method employed involved (1) calculating the volume, V_e, of the ellipsoidal cavity best suited to a given molecule, (2) defining an arbitrary sphere whose volume V_s equals V_e, and (3) finding the radius of the sphere whose volume is V_s. This latter radius, r_c^{min}, can be ~10−30% smaller than r_c^{max}, and in many cases exceeds the bounds of a realistic number. Nevertheless, it allows us to estimate a lower limit for IP^{sol}. The data shown in Table 1 derive from cavity radii that are uniformally 10% smaller than r_c^{max}.

Irrespective of the r_c value employed for a given molecule M, plots of k_r^{a-X}/n^2 against IP^{sol} (Figure 3) are not significantly different from that of k_r^{a-X}/n^2 against IP^{gas}. Moreover, all plots of k_r^{a-X}/n^2 against IP show significantly poorer correlations than, for example, that in Figure 1. The latter, in fact, represents the best correlation thus far identified between k_r^{a-X} and a solvent parameter. Thus, it appears that the solvent effects on k_r^{a-X} most likely derive from phenomena other than a CT interaction.

To find an explanation for the general trend observed in Figures 2 and 3, it is instructive to plot the refractive index against IP^{gas} for this same group of solvents (Figure 4). Upon examination of this latter plot, it is apparent that the k_r^{a-X}/n^2 vs IP plots reflect a transitive effect that derives from relationships between (1) k_r^{a-X}/n^2 and n and (2) n and IP.

Because Figures 1−4 are key to our arguments, it is important to discuss specific features of these plots in light of the corresponding plots presented by proponents of the CT-coupling postulate:[5,19]

TABLE 2: Additional Rate Constants, k_r^{a-X}, for the Radiative Deactivation of $O_2(a^1\Delta_g)$

solvent	n	IP^{gas} (kJ/mol)	k_r^{a-X} (s^{-1})
H_2O	1.333	1217	0.11[a]
diethyl ether	1.353	917.6	0.62[b]
n-pentane	1.358	998.6	0.47[d]
ethanol	1.360	1010	0.50[b]
formic acid	1.370	1093	0.25[d]
n-hexane	1.375	977.4	0.60[d]
C_6F_6	1.377	955.8	0.51[c]
1-propanol	1.384	986.1	0.47[e]
propionic acid	1.386	1016	0.79[d]
acetic anhydride	1.390	(~965)	0.53[d]
2-nitropropane	1.394	1033	0.19[d]
2-butanol	1.398	953.3	0.57[b]
1-butanol	1.399	970.7	0.44[e]
C_6F_5Cl	1.421	937.9	0.89[c]
N,*N*-dimethylformamide	1.431	880.9	0.63[b]
1,2-dichloroethane	1.445	1065	0.75[d]
C_6F_5Br	1.449	923.4	1.25[c]
CCl_4	1.460	1107	1.10[f]
toluene-d_8	1.493	851.0	1.47[d]
p-xylene	1.495	814.4	1.70[d]
C_6F_5I	1.497	920.5	1.23[c]
1,2,4-trimethylbenzene	1.504	798.0	2.00[d]
anisole	1.516	792.2	1.80[d]
1,3-dimethoxybenzene	1.524	786.4	1.90[d]
p-chloroanisole	1.535	796.0	2.20[d]
p-bromoanisole	1.564	785.4	1.90[d]
phenyl ether	1.579	780.6	2.00[d]

[a] Average of three independent numbers.[3,5,6] [b] Darmanyan.[5] [c] Schmidt and Afshari.[3] [d] Darmanyan.[19] [e] Average of two independent numbers.[5,37] [f] Schmidt and Bodesheim.[8]

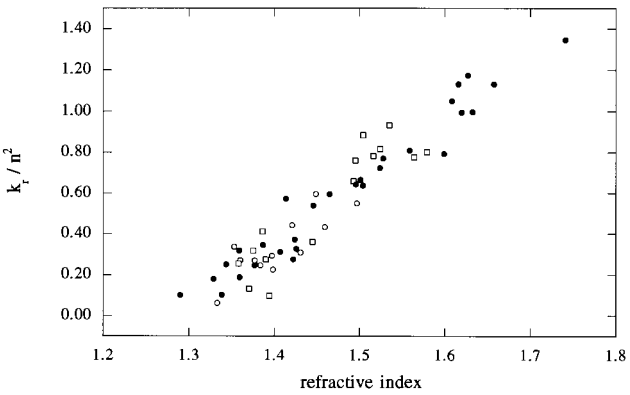

Figure 5. Plot of k_r^{a-X}/n^2 vs the solvent refractive index, n. Data from Table 1, which are also shown in Figure 1, are denoted with solid circles (●). Additional data are from Table 2 and represent experiments performed by Darmanyan[19] (□) as well as others[3,5,6] (○).

(1) We compare plots of k_r^{a-X}/n^2 vs n with plots of k_r^{a-X}/n^2 vs IP, not $\log(k_r^{a-X}/n^2)$ vs IP. We see no physical reason to take the logarithm of the ordinate other than to yield a plot that shows less scatter in the data.

(2) A desirable feature of the k_r^{a-X} data listed in Table 1 and used in Figures 1−3 is that the numbers, in general, are an average of data obtained by more than one investigator.[2] This is an important consideration because experiments to quantify k_r^{a-X} are quite susceptible to error. Although a significant number of points have been used in Figures 1−3, k_r^{a-X} data are nevertheless available for more solvents. Listed in Table 2 are values of k_r^{a-X} for an additional 27 solvents, each of which principally reflects the work of a single investigator. Despite the obvious limitations of this latter data set, plots of k_r^{a-X}/n^2 vs n and k_r^{a-X}/n^2 vs IP^{gas} that include all 56 solvents (Figures

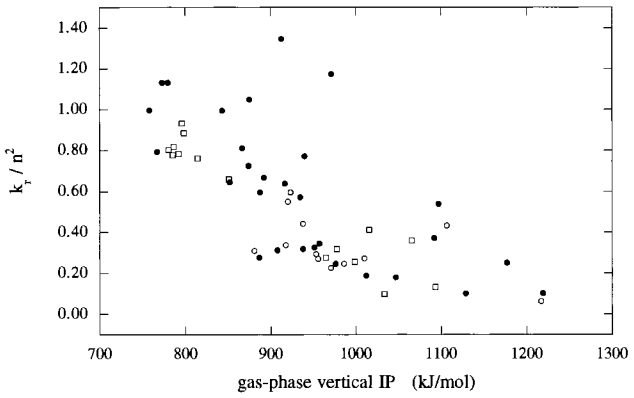

Figure 6. Plot of k_r^{a-X}/n^2 against the gas-phase vertical ionization potential, IP^{gas}, for the respective solvents. Data from Table 1, which are also shown in Figure 2, are denoted with solid circles (●). Additional data are from Table 2 and represent experiments performed by Darmanyan[19] (□) as well as others[3,5,6] (○).

5−6) are consistent with the corresponding plots shown in Figures 1 and 2.[33]

(3) Use of the London formula to quantify dispersion interactions between oxygen and the solvent can have large errors. Specifically, we have recently shown that contrary to traditional expectations, the polarizability of $O_2(a^1\Delta_g)$, α_a, is in fact not significantly larger than the polarizability of $O_2(X^3\Sigma_g^-)$, α_X.[34] Rather, α_a is quite similar to α_X and, depending on the solvent, can even be *smaller* than α_X. This fact, coupled with uncertainties in the $M-O_2$ interaction radius, demand that caution be exercised in drawing conclusions from plots in which the dispersion energy is a variable. Rather, it seems more prudent at this stage to simply identify solvent parameters with which changes in k_r^{a-X} best correlate.

At present, the most promising model that accounts for the effect of solvent on k_r^{a-X} is that of Minaev.[35] The principal postulate is that by virtue of a spin−orbit interaction that mixes $O_2(b^1\Sigma_g^+)$ with $O_2(X^3\Sigma_g^-)$, the $a-X$ transition can steal intensity from the $b-a$ transition. The $b-a$ transition is proposed to gain intensity via a solvent-dependent disruption of the cylindrical symmetry in oxygen. Specifically, upon interaction with the perturbing molecule M, a distinction is made between oxygen's normally degenerate π_y and π_x antibonding orbitals which, in turn, gives rise to a dipolar component in the $b-a$ transition. In comparison to the unperturbed transition, which is allowed only as an electric quadrupole process, the collision-induced electric dipole character causes a significant increase in the $b-a$ transition probability.[36] It is reasonable to expect that the magnitude of this induced dipole would increase with an increase in the optical polarizability of M, which is consistent with the correlation shown in Figures 1 and 5.

Conclusions

Arguments have been presented to indicate that CT interactions are not likely to be a principal factor in the effect of solvent on the $a-X$ transition probability. The general trend in plots of k_r^{a-X}/n^2 vs IP appears to derive from other phenomena via a transitive effect. The data indicate that the electronic response of the solvent (e.g., optical polarizability) is a key parameter that must be considered in the development of models that account for this remarkable solvent effect.

Acknowledgment. This work was supported by grants from (1) the U.S. National Science Foundation (Grant No. CHE-9402145), (2) the Danish Natural Science Research Council (Grant No. 9601705), and (3) the SNF center for Molecular Dynamics and Laser Chemistry. The authors thank Dr. Alexander Darmanyan for allowing us to use his data. The authors also thank Steen Jakobsen for assistance in the early stages of this project.

References and Notes

(1) Scurlock, R. D.; Ogilby, P. R. *J. Phys. Chem.* **1987**, *91*, 4599−4602.
(2) Scurlock, R. D.; Nonell, S.; Braslavsky, S. E.; Ogilby, P. R. *J. Phys. Chem.* **1995**, *99*, 3521−3526.
(3) Schmidt, R.; Afshari, E. *J. Phys. Chem.* **1990**, *94*, 4377−4378.
(4) Gorman, A. A.; Krasnovsky, A. A.; Rodgers, M. A. J. *J. Phys. Chem.* **1991**, *95*, 598−601.
(5) Darmanyan, A. P. *Chem. Phys. Lett.* **1993**, *215*, 477−482.
(6) Losev, A. P.; Nichiporovich, I. N.; Byteva, I. M.; Drozdov, N. N.; Al Jghgami, I. F. *Chem. Phys. Lett.* **1991**, *181*, 45−50.
(7) Gorman, A. A.; Hamblett, I.; Lambert, C.; Prescott, A. L.; Rodgers, M. A. J.; Spence, H. M. *J. Am. Chem. Soc.* **1987**, *109*, 3091−3097.
(8) Schmidt, R.; Bodesheim, M. *J. Phys. Chem.* **1995**, *99*, 15919−15924.
(9) Scurlock, R. D.; Ogilby, P. R. *J. Phys. Chem.* **1989**, *93*, 5493−5500.
(10) Kristiansen, M.; Scurlock, R. D.; Iu, K.-K.; Ogilby, P. R. *J. Phys. Chem.* **1991**, *95*, 5190−5197.
(11) Tsubomura, H.; Mulliken, R. S. *J. Am. Chem. Soc.* **1960**, *82*, 5966−5974.
(12) Kawaoka, K.; Khan, A. U.; Kearns, D. R. *J. Chem. Phys.* **1967**, *46*, 1842−1853.
(13) Clennan, E. L.; Noe, L. J.; Szneler, E.; Wen, T. *J. Am. Chem. Soc.* **1990**, *112*, 5080−5085.
(14) Garner, A.; Wilkinson, F. *Chem. Phys. Lett.* **1977**, *45*, 432−435.
(15) Redmond, R. W.; Braslavsky, S. E. *Chem. Phys. Lett.* **1988**, *148*, 523−529.
(16) Clennan, E. L.; Noe, L. J.; Wen, T.; Szneler, E. *J. Org. Chem.* **1989**, *54*, 3581−3584.
(17) Young, R. H.; Martin, R. L.; Feriozi, D.; Brewer, D.; Kayser, R. *Photochem. Photobiol.* **1973**, *17*, 233−244.
(18) Thomas, M. J.; Foote, C. S. *Photochem. Photobiol.* **1978**, *27*, 683−693.
(19) Darmanyan, A. P. *J. Phys. Chem. A* **1998**, *102*, 9833.
(20) Strickler, S. J.; Berg, R. A. *J. Chem. Phys.* **1962**, *37*, 814−822.
(21) Ionization potentials were obtained from three sources. (a) *Handbook of Chemistry and Physics*, 74th ed.; Lide, D. R., Ed.; CRC Press: Boca Raton, FL, 1994. (b) Lias, S. G.; Bartmess, J. E.; Liebman, J. F.; Holmes, J. L.; Levin, R. D.; Mallard, W. G. *J. Phys. Chem. Ref. Data* **1988**, *17*, 1−861. (c) NIST Internet Web Book (http://webbook.nist.gov/) .
(22) Ŝiegbahn, H. *J. Phys. Chem.* **1985**, *89*, 897−909.
(23) Ågren, H.; Medina-Llanos, C.; Mikkelsen, K. V. *Chem. Phys.* **1987**, *115*, 43−51.
(24) Barton, A. F. M. *Handbook of Solubility Parameters and Other Cohesion Parameters*, 2nd ed.; CRC Press: Boca Raton, FL, 1991.
(25) Billing, G. D.; Mikkelsen, K. V. *Advanced Molecular Dynamics and Chemical Kinetics*; John Wiley and Sons: New York, 1997.
(26) Mikkelsen, K. V.; Jørgensen, P.; Jensen, H. J. A. *J. Chem. Phys.* **1994**, *100*, 6597−6607.
(27) Mikkelsen, K. V.; Cesar, A.; Aagren, H.; Jensen, H. J. A. *J. Chem. Phys.* **1995**, *103*, 9010−9023.
(28) Mikkelsen, K. V.; Sylvester-Hvid, K. O. *J. Phys. Chem.* **1996**, *100*, 9116−9126.
(29) Logunov, S. L.; Rodgers, M. A. J. *J. Phys. Chem.* **1993**, *97*, 5643−5648.
(30) McGarvey, D. J.; Wilkinson, F.; Worrall, D. R.; Hobley, J.; Shaikh, W. *Chem. Phys. Lett.* **1993**, *202*, 528−534.
(31) Kuriyama, Y.; Ogilby, P. R.; Mikkelsen, K. V. *J. Phys. Chem.* **1994**, *98*, 11918−11923.
(32) Wave Function, Inc.: Irvine, CA, Version 4.1.
(33) Although data for 56 solvents are shown, we have specifically not included k_r^{a-X} values measured by Darmanyan[19] in mesitylene, CH_2Br_2, and formamide. We suggest that additional experiments need to be performed in these solvents. On the other hand, of the solvents considered in our study, CCl_4 and $CHCl_3$ were excluded in Darmanyan's analysis.[19]
(34) Poulsen, T. D.; Ogilby, P. R.; Mikkelsen, K. V. *J. Phys. Chem. A* **1998**, *102*, 8970.
(35) Minaev, B. F.; Lunell, S.; Kobzev, G. I. *J. Mol. Struct. (THEOCHEM)* **1993**, *284*, 1−9.
(36) Herzberg, G. *Molecular Spectra and Molecular Structure. I. Spectra of Diatomic Molecules*, 2nd ed.; Van Nostrand Reinhold: New York, 1950.
(37) Darmanyan, A. P.; Foote, C. S. *J. Phys. Chem.* **1993**, *97*, 5032−5035.